Journal of Alloys and Compounds 503 (2010) 490–493

Contents lists available at ScienceDirect

Journal of Alloys and Compounds

journal homepage: www.elsevier.com/locate/jallcom

# Thermoelectric properties of n-type $CoSb_3$ fabricated with high pressure sintering

Jianjun Zhang, Bo Xu*, Fengrong Yu, Dongli Yu, Zhongyuan Liu, Julong He, Yongjun Tian*

*State Key Laboratory of Metastable Materials Science and Technology, Yanshan University, Qinhuangdao, Hebei 066004, China*

ARTICLE INFO

*Article history:*
Received 18 December 2009
Received in revised form 6 May 2010
Accepted 8 May 2010
Available online 21 May 2010

*Keywords:*
Skutterudite compounds
HPS
Anneal
Thermoelectric properties

ABSTRACT

Highly densified single-phase n-type polycrystalline $CoSb_3$ samples were prepared with high pressure sintering method followed by annealing under argon environment. The microstructure and thermoelectric properties of the samples were characterized. The Hall coefficient measurements indicate that the majority carrier concentration is about $10^{19}$ $cm^{-3}$ at 300 K for the annealed samples. The dimensionless figure of merit, ZT, maintains a relatively high value over a wide range of measured temperature. The maximum ZT of 0.15 is achieved at 523 K for the sample annealed at 773 K.



## 1. Introduction

Thermoelectric materials have been extensively studied nowadays due to the increasing need for replacement energy as well as the requirement of reducing the environmental deterioration from the greenhouse effect [1–5]. However, the low conversion efficiency has set a severe barrier for large-scale commercial applications [6]. The performance of thermoelectric materials is characterized by the dimensionless figure of merit, $ZT = S^2\sigma T/\kappa$, where $S$, $\sigma$, $T$, and $\kappa$ are the Seebeck coefficient, electrical conductivity, temperature, and thermal conductivity, respectively. A good thermoelectric material should possess large Seebeck coefficient and electrical conductivity as well as low thermal conductivity [7]. Materials with skutterudite structure are good candidates for improving these thermoelectric properties [8]. The binary skutterudite compounds have a cubic structure with space group of *Im*-3. The structure can be denoted as $AX_3$, where A is Co, Rh or Ir, and X is Sb, As or P, etc. There are two cages per unit cell where extrinsic atoms can be accommodated as rattling atoms to scatter phonons, leading to the so-called filled skutterudite structure with enhanced ZT through phonon-glass electron-crystal approach [9]. Numerous researches have been carried out on filled skutterudite materials and promising progresses have been made [10–15].

$CoSb_3$ is one of the most studied skutterudite materials as well as the mother compound for extrinsic atom filling. Spark plasma sintering (SPS), arc melting and hot pressing have been employed to prepare $CoSb_3$ bulk samples. Samples synthesized with SPS method have well-controlled grain size and reduced thermal conductivity, but ZT is limited by the relatively low power factor [16]. Hot pressing method can produce samples with fine-grained structure and high density (relative density larger than 90%), and ZT is enhanced due to improved electrical conductivity [17]. Novel chemical alloying route was also used to prepare nanocrystalline $CoSb_3$ samples with high grain boundary density [18]. The thermal conductivity is reduced in this case, but the sample density is low (relative density in the range of 65.71–74.48%). Recently, it was shown that high pressure sintering (HPS) technique can effectively increase material density and improve thermoelectric properties, especially the electrical conductivity [19–21]. The electrical resistivity of PbTe decreases sharply with increasing synthesis pressure from ambient pressure to 3.2 GPa [21]. For the p-type $CoSb_3$ samples synthesized under high pressure and high temperature with the grain size of micrometers, ZT was increased to 0.17 [20]. It is anticipated that HPS can also be used to fabricate n-type bulk $CoSb_3$ with improved thermoelectric properties.

Here, we report n-type $CoSb_3$ compounds prepared with HPS method. The thermoelectric properties of HPS samples before and after annealing were systematically studied. Relatively high power factors ($S^2\sigma$) were achieved for the annealed samples over a wide temperature range. The effectiveness of HPS technique in skutterudite $CoSb_3$ fabrication has been demonstrated.

## 2. Experimental details

In our experiments, Co powders (99.99%) and Sb powders (99.999%) were mixed according to the stoichiometric ratio (1:3.1). Extra Sb was added to compensate the loss at high temperature due to its high vapor pressure [22]. The mixed powders were put into carbon capsules, loaded into furnace, and pre-sintered at 973 K for 20 h under flowing argon protection to produce polycrystalline $CoSb_3$. The synthesized product was ground into powders for high pressure sintering at 4 GPa and 873 K

* Corresponding authors.
*E-mail addresses:* bxu@ysu.edu.cn (B. Xu), fhcl@ysu.edu.cn (Y. Tian).

0925-8388/$ – see front matter © 2010 Elsevier B.V. All rights reserved.
doi:10.1016/j.jallcom.2010.05.039

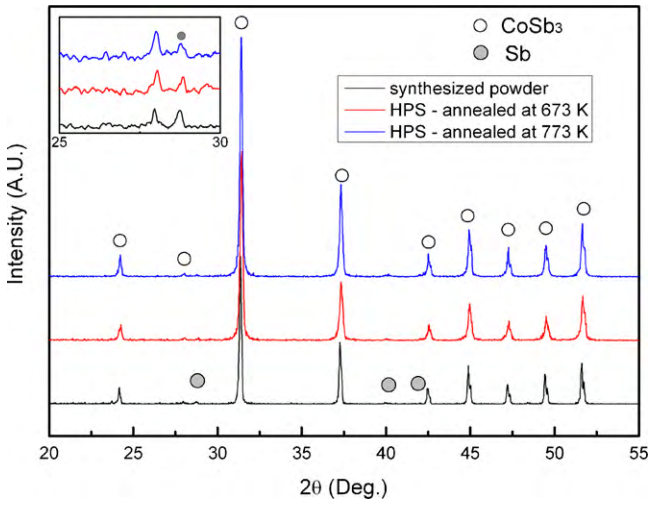


**Fig. 1.** XRD patterns of pre-sintering powders and annealed HPS samples.

for 15 min. The pressure was chosen to ensure the high density in the fabricated sample. In the end of the HPS process, samples were quenched to room temperature prior to releasing the applied pressure. The HPS samples were then heated slowly (5 K/min) to 673 K (or 773 K) and kept at the temperature for 5 min to release the residual stress under Ar protection. The annealed and unannealed HPS samples were cut into rectangular blocks (2 mm × 2 mm × 8 mm) and the disks (Ø 8 mm × 1 mm) for the electrical transport measurements and thermal conductivity measurements, respectively.

The structure of polycrystalline $CoSb_3$ was characterized by X-ray diffraction (Rigaku, D/MAX/2500/PC) with Cu Kα. The sample density was measured with the Archimedes method. The Seebeck coefficient and electrical conductivity were measured with a ZEM-3 (Ulvac-Riko, Inc.) apparatus, and the thermal conductivity was measured with a TC-7000H (Ulvac-Riko, Inc.) apparatus.

## 3. Results and discussion

The X-ray diffraction patterns of the pre-sintered $CoSb_3$ powders as well as the annealed HPS samples are shown in Fig. 1. The main phase is skutterudite $CoSb_3$. According to the XRD patterns, there is some residual Sb existing in the pre-sintered $CoSb_3$ powders and the annealed samples. As indicated by the magnified XRD patterns in the inset of Fig. 1, the reflection from the Sb becomes weaker for the annealed HPS samples, indicating smaller amount of residual Sb in these samples.

The density of HPS samples before annealing is 7.674 g cm$^{-3}$, which is higher than the theoretical density of 7.639 g cm$^{-3}$. HPS technique thus provides us an effective way to fabricate highly densified samples. The density of HPS samples annealed at 673 K and 773 K is lowered to 7.585 g cm$^{-3}$ and 7.396 g cm$^{-3}$, respectively, indicating a volume expansion during the annealing. As shown in Fig. 2, the SEM micrographs of the fractured surfaces from annealed HPS samples manifest grains with the size of several micrometers. Obviously, there are more pores and micro-cracks in the sample annealed at 773 K, which is consistent with the measured sample densities. The pores and micro-cracks as well as the decrease of sample density can be attributed to the stress releasing process occurring at elevated temperatures.

The Hall coefficients of the annealed HPS samples are shown in Fig. 3. The negative value indicates n-type conduction in $CoSb_3$ bulks. For both samples, the Hall coefficients decrease with increasing temperature due to the enhanced thermal vibration at high temperature [23]. The measured carrier concentrations at 300 K are $1.7 \times 10^{19}$ cm$^{-3}$ and $1.0 \times 10^{19}$ cm$^{-3}$ for the samples annealed at 673 K and 773 K, respectively. The lower carrier concentration in the sample annealed at 773 K may connect to the lower density of Sb vacancy, which is consistent with the lower residual Sb in this sample (Fig. 1).

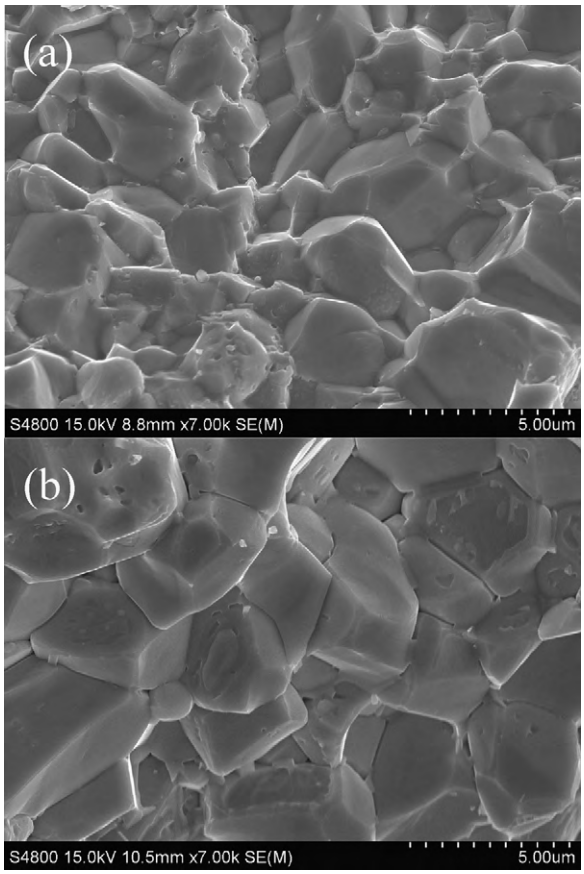


**Fig. 2.** SEM images of the fractured surfaces for (a) the HPS sample annealed at 673 K and (b) the HPS sample annealed at 773 K.

The temperature dependences of thermoelectric properties are shown in Fig. 4 for both annealed and unannealed HPS samples. Obviously, the Seebeck coefficient is significantly enhanced after annealing and maintains a relative high value for the measured temperature range. The variation tendency of the Seebeck coefficient for the annealed samples is consistent with that of the Hall coefficient: the sample annealed at 773 K possesses larger Hall coefficient and Seebeck coefficient. In some $CoSb_3$ samples, the Seebeck coefficient can change sign from negative to positive as temperature increased [16,23,24], resulting in the diminishing of

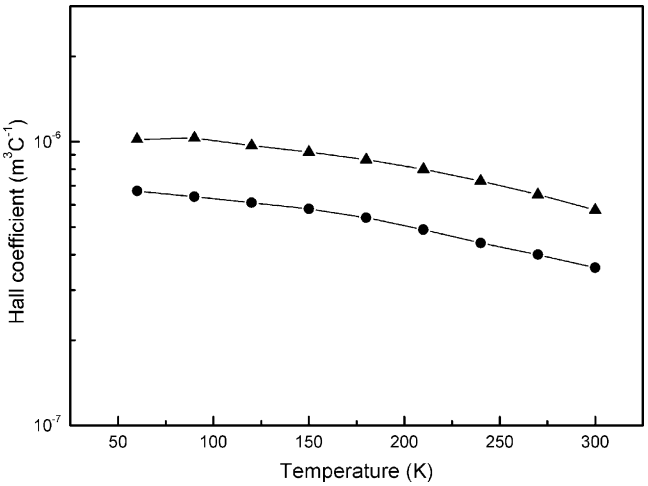


**Fig. 3.** The Hall coefficient of annealed HPS samples measured from 60 K to 300 K (-●- sample annealed at 673 K, -▲- sample annealed at 773 K).

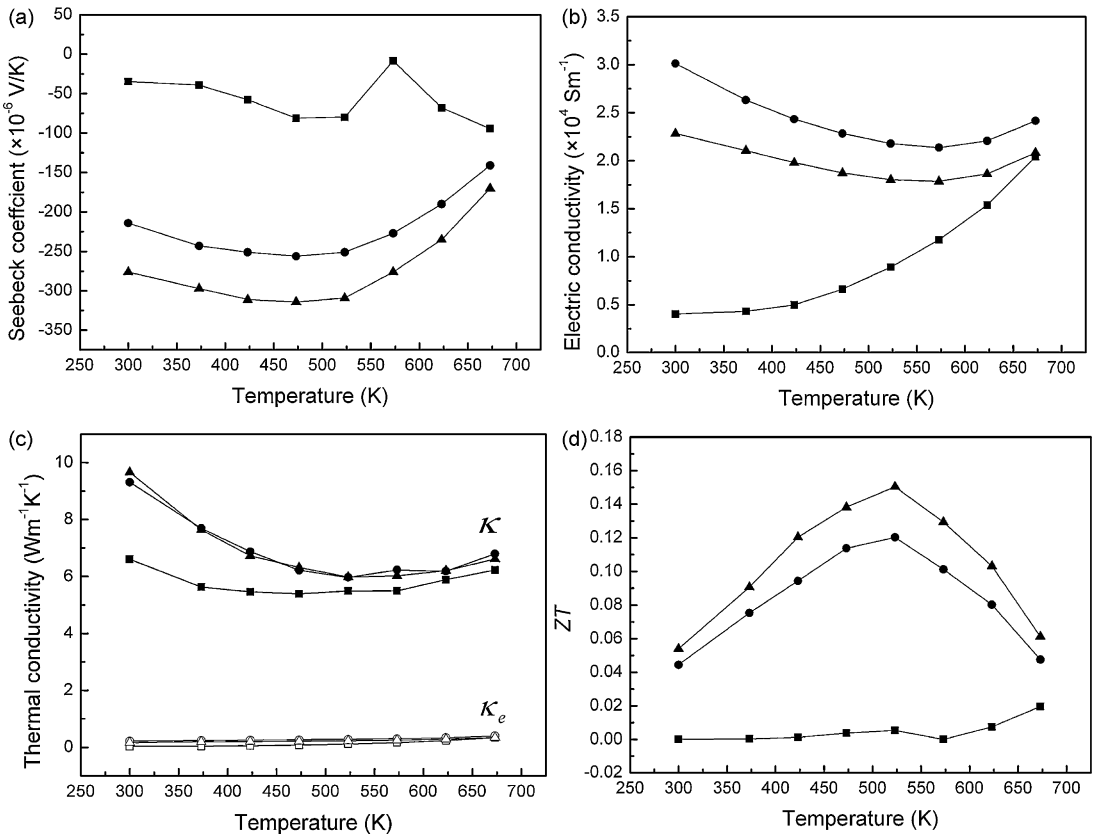


**Fig. 4.** The temperature dependencies of (a) the Seebeck coefficient, (b) electrical conductivity, (c) thermal conductivity, and (d) the dimensionless figure of merit ZT (-■- sample without annealing, -●- sample annealed at 673 K, and -▲- sample annealed at 773 K). $\kappa_e$ is also shown in (c) (-□- sample without annealing, -○- sample annealed at 673 K, and -△- sample annealed at 773 K).

thermoelectric properties in the corresponding temperature range. In our experiments, the two annealed $CoSb_3$ samples exhibit n-type conduction for the temperature up to 700 K. We do notice a decreasing Seebeck coefficient when temperature is above 500 K, which can be attributed to the increasing contribution from minority carriers (holes) at high temperature.

The temperature dependence of the electrical conductivity is shown in Fig. 4(b). Similar to the Seebeck coefficient, the electrical conductivity of the annealed HPS samples are highly improved compared with the unannealed sample near room temperature. The electrical conductivity of the unannealed sample shows typical characters of semiconductor. For the annealed samples, the electrical conductivity is controlled by the electrons and decreasing with increasing temperature from room temperature to 550 K. Above 550 K, when an increasing number of holes are thermally excited, the electrical conductivity increases. The temperature dependence of electrical conductivity is consistent with that of the Seebeck coefficient for the annealed samples. Moreover, the sample annealed at 773 K possesses a lower electrical conductivity than that of the sample annealed at 673 K, which is also consistent with the variation tendency in the Hall coefficient and Seebeck coefficient. The electrical conductivity of the annealed HPS sample is higher than that of the $CoSb_3$ samples sintered under vacuum [24]. This improvement results from the high sample density and optimization of transport property in the HPS samples.

The temperature dependence of the thermal conductivity is shown in Fig. 4(c). The total thermal conductivity can be expressed as $\kappa = \kappa_L + \kappa_e$, where $\kappa_L$ and $\kappa_e$ are the lattice thermal conductivity and electronic thermal conductivity. $\kappa_e$ can be calculated with Wiedemann–Franz law, $\kappa_e = L\sigma T$, where $L = 2.45 \times 10^{-8}\,V^2\,K^{-2}$ is the Lorenz number. Obviously, the lattice thermal conductivity dominates in our HPS samples. In polycrystalline materials, grain boundary and porosity would contribute to reduce the thermal conductivity [18]. Our samples annealed at different temperatures have similar grain size and sample density, so the similarity in thermal conductivity is expected. It is noted that the thermal conductivity is increasing at high temperature. This increase can be attributed to the increasing contribution to the thermal conductivity from bipolar effect at high temperature [25]. The thermal conductivities of the annealed samples are slightly higher than that of the unannealed sample, which may be attributed to the increase of grain size after annealing.

The dimensionless figure of merit ZT as a function of temperature is calculated and demonstrated in Fig. 4(d). Due to the great improvements in the Seebeck coefficient and electrical conductivity, ZT is highly increased after annealing. The sample annealed at 673 K has the maximum ZT = 0.12 at 523 K and the sample annealed at 773 K has the maximum ZT = 0.15 at the same temperature. In addition, ZT of the annealed HPS samples maintains a relatively high value over a wide range of temperature.

The thermoelectric property improvement in our samples is mainly due to the enhancement of the power factor. Another advantage of HPS method is the presence of high pressure can hinder the coarsening of nanocrystalline grains during sintering. It is possible to fabricate highly densified nanostructured thermoelectric materials with few atomic defects and small grain size using this HPS method, leading to significant decrease in thermal conductivity. Such improvement is observed in bulk nanostructured $Bi_2Te_3$ samples produced with HPS method, as we will report later elsewhere. By optimizing the thermal conductivity with introducing atoms to the cage as "rattle" to scatter phonons [26] and increasing grain boundary density with nanostructured $CoSb_3$ [27], a further enhancement in ZT can be expected. Continuous researches based on these considerations are undertaken now.

## 4. Conclusions

Highly densified n-type skutterudite $CoSb_3$ samples were synthesized with high pressure sintering method at 4 GPa and 873 K. The ZT of the 773 K annealed HPS sample reaches 0.15 at 523 K and maintains a relatively high value between 400 K and 650 K. In the annealed sample, the Seebeck coefficient and electrical conductivity show similar temperature dependence which can be accounted for by the carrier concentration. The power factor, $S^2\sigma$, is greatly enhanced with the HPS method compared with other ambient pressure methods. A further improvement in thermal conductivity as well as ZT is expected by decreasing the grain size and/or incorporating extrinsic atoms into the skutterudite cages.

## Acknowledgements

This work was supported by NSFC (Grant No. 50821001), PCSIRT (Grant No. IRT 0650), and NBRPC (Grant No. 2005CB724400).

## References

[1] L.E. Bell, Science 321 (2008) 1457–1461.
[2] D.J. Singh, I. Terasaki, Nat. Mater. 7 (2008) 616–617.
[3] T. Tritt, M. Subramanian, MRS Bull. 31 (2006) 188–194.
[4] Y. Lan, A.J. Minnich, G. Chen, Z. Ren, Adv. Funct. Mater. 20 (2010) 357–376.
[5] J.R. Sootsman, D.Y. Chung, M.G. Kanatzidis, Angew. Chem. Int. Ed. 48 (2009) 8616–8639.
[6] C.B. Vining, Nat. Mater. 8 (2009) 83–85.
[7] G. Casati, C. Mejía-Monasterio, T. Prosen, Phys. Rev. Lett. 101 (2008) 016601.
[8] G.A. Slack, V.G. Tsoukala, J. Appl. Phys. 76 (1994) 1665–1671.
[9] G.A. Slack, in: D.M. Rowe (Ed.), Thermoelectric Handbook, CRC, Boca Raton, FL, 1995, p. 407.
[10] J.R. Salvador, J. Yang, X. Shi, H. Wang, A.A. Wereszczak, H. Kong, C. Uher, Phil. Mag. 89 (2009) 1517–1534.
[11] G. Nolas, D. Morelli, T. Tritt, Annu. Rev. Mater. Sci. 29 (1999) 89–116.
[12] L. Yang, J. Wu, L. Zhang, J. Alloys Compd. 364 (2004) 83–88.
[13] W. Zhao, P. Wei, Q. Zhang, C. Dong, L. Liu, X. Tang, J. Am. Chem. Soc. 131 (2009) 3713–3720.
[14] K. Yang, H. Cheng, H.H. Hng, J. Ma, J.L. Mi, X.B. Zhao, T.J. Zhu, Y.B. Zhang, J. Alloys Compd. 467 (2009) 528–532.
[15] K. Mangersnes, O.M. Lovvik, O. Prytz, New J. Phys. 10 (2008) 053004.
[16] J.X. Zhang, Q.M. Lu, K.G. Liu, L. Zhang, M.L. Zhou, Mater. Lett. 58 (2004) 1981–1984.
[17] Z.M. He, C. Stiewe, D. Platzek, G. Karpinski, E. Müller, S.H. Li, M. Toprak, M. Muhammed, J. Appl. Phys. 101 (2007) 053713.
[18] M.S. Toprak, C. Stiewe, D. Platzek, S. Williams, L. Bertini, E. Müller, C. Gatti, Y. Zhang, M. Rowe, M. Muhammed, Adv. Funct. Mater. 14 (2004) 1189–1196.
[19] T.C. Su, X.P. Jia, H.A. Ma, Y.P. Jiang, N. Dong, L. Deng, X.B. Zhao, T.J. Zhu, C. Wei, J. Alloys Compd. 468 (2009) 410–413.
[20] N. Dong, X. Jia, T.C. Su, F.R. Yu, Y.J. Tian, Y.P. Jiang, L. Deng, H.A. Ma, J. Alloys Compd. 480 (2009) 882–884.
[21] P.W. Zhu, X. Jia, H.Y. Chen, W.L. Guo, L.X. Chen, D.M. Li, H.A. Ma, G.Z. Ren, G.T. Zou, Solid State Commun. 123 (2002) 43–47.
[22] X.Y. Zhao, X. Shi, L.D. Chen, W.Q. Zhang, W.B. Zhang, Y.Z. Pei, J. Appl. Phys. 99 (2006) 053711.
[23] X.Y. Li, L.D. Chen, J.F. Fan, W.B. Zhang, T. Kawahara, T. Hirai, J. Appl. Phys. 98 (2005) 083702.
[24] Y. Kawaharada, K. Kurosaki, M. Uno, Yamanaka, J. Alloys Compd. 315 (2001) 193–197.
[25] F.R. Yu, J.J. Zhang, D.L. Yu, J.L. He, Z.Y. Liu, B. Xu, Y.J. Tian, J. Appl. Phys. 105 (2009) 094303.
[26] G.S. Nolas, G. Fowler, J. Yang, J. Appl. Phys. 100 (2006) 043705.
[27] J.L. Mi, T.J. Zhu, X.B. Zhao, J. Ma, J. Appl. Phys. 101 (2007) 054314.